

Using GCxGC and the Agilent 7200 GC/Q-TOF for an Untargeted Metabolomics Study of the Fungal Rice Pathogen *Magnaporthe oryzae*

Application Note

Metabolomics

Authors

William C. Ledford,
Margarita Marroquin-Guzman,
and Richard A. Wilson
Department of Plant Pathology
University of Nebraska at Lincoln
Lincoln, NE
USA

Edward B. Ledford and Zhanpin Wu
Zoex Corporation
Houston, TX
USA

Qingping Tao and
Stephen E. Reichenbach
GC Image LLC
Lincoln, NE
USA

Sofia Nieto
Agilent Technologies, Inc.
Santa Clara, CA

Abstract

Comprehensive two-dimensional gas chromatography (GCxGC) provides the superior chromatographic resolution that, when used in combination with accurate mass, high resolution mass spectrometry (MS), greatly facilitates compound identification and structure elucidation in complex matrices. An untargeted metabolomics study using GCxGC/Q-TOF MS on the Agilent 7890B GC equipped with a Zoex ZX2 thermal modulator and an Agilent 7200 GC/Q-TOF identified several metabolites that may play an important role in the pathogenesis of the rice blast fungus *M. oryzae*.



Agilent Technologies

Introduction

Rice blast disease caused by the fungus *Magnaporthe oryzae* is the most serious disease of cultivated rice and a global food security threat, causing 10 to 30 % losses in rice crops each year [1,2]. Changing climates enable its spread into new areas. There is, therefore, an urgent need for environmentally sustainable rice blast control strategies. An in-depth understanding of the *M. oryzae* infection process is required to enable such strategies.

In addition to its importance as a critical plant pathogen, *M. oryzae* shares many characteristics associated with other important cereal pathogens, making it a good model organism for studies that could lead to broad-spectrum crop disease control [2]. These pathogens have a common mechanism of infection that uses a specialized cell called an appressorium which forms on the leaf surface and generates enormous hydrostatic turgor, forcing a penetration hypha into underlying epidermal cells [1].

The metabolic strategies used by *M. oryzae* to colonize rice cells are largely unknown. This application note describes a study focused on understanding nutrient acquisition and use in *M. oryzae* that may help to shed light on the infection process, and identify new avenues for effective disease management. This study compared metabolomes of a wildtype (WT) strain (Guy11) of *M. oryzae* to nonpathogenic mutant strains resulting from the deletion of key metabolic regulatory genes encoding a central nitrogen regulator ($\Delta nut1$), a carbon regulator ($\Delta mdt1$), and a carbon-nitrogen metabolic integrator ($\Delta tps1$) [3].

Comprehensive two-dimensional gas chromatography (GCxGC) was combined with high resolution accurate mass quadrupole time-of-flight mass spectrometry (Q-TOF MS) to compare metabolomes of a WT isolate of *M. oryzae* to the three nonpathogenic mutant strains. This approach revealed numerous metabolites that may play a role in the pathogenesis of *M. oryzae*.

Experimental

Instruments

This study was performed using an Agilent 7890B GC system coupled to an Agilent 7200 series GC/Q-TOF system (Figure 1). The GCxGC system (Figures 1 and 2) used a thermal loop modulator (Model ZX2, Zoex Corporation, Houston, TX). Analyte bands eluting from the primary column were cryogenically accumulated, focused, and remobilized every 6.8 seconds (modulation period), thereby injecting a series of “cuts” from the first column onto the second, from which secondary chromatograms eluted within each modulation period. Figure 2 shows a photograph of the thermal modulator. The Q-TOF MS acquired accurate mass, high resolution spectra of the secondary column effluent at a rate of 50 full scan acquisition spectra per second, in both electron ionization (EI) and positive chemical ionization (PCI) modes. The instrument conditions are listed in Table 1, and a schematic of the GCxGC configuration is shown in Figure 3.

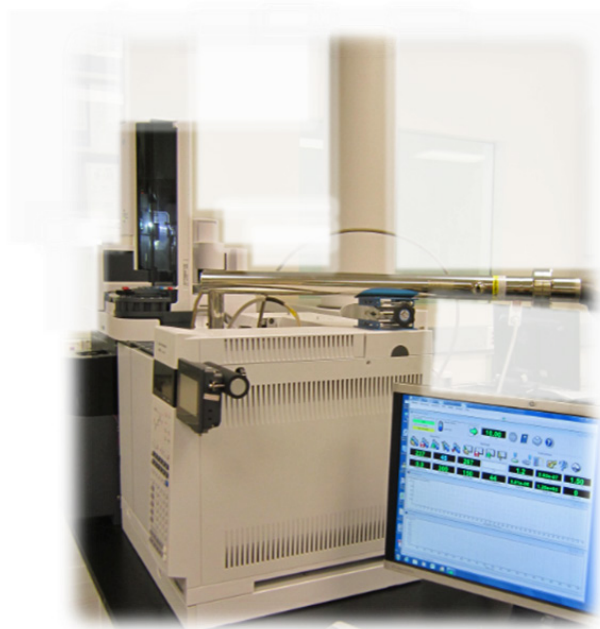


Figure 1. Agilent 7890B GC system equipped with Zoex ZX2 thermal modulator and coupled to an Agilent 7200 series GC/Q-TOF system.

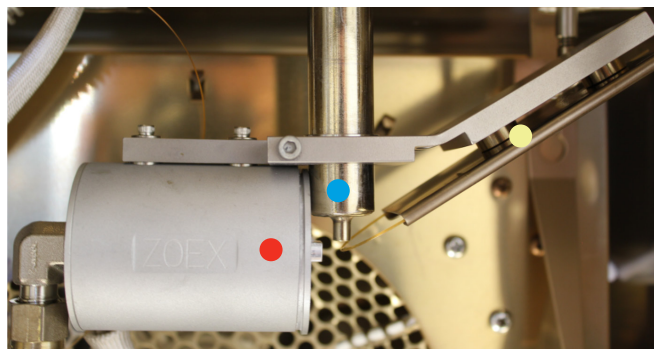


Figure 2. Photograph of the Thermal Modulator inside the oven of the Agilent 7890B GC. The cold jet (blue dot) is used to collect material eluting from the first GC column into the loop. Every few seconds, the hot jet (red dot) is pulsed on to pass collected material from the loop to the second GC column. The yellow dot shows the location of the loop holder.

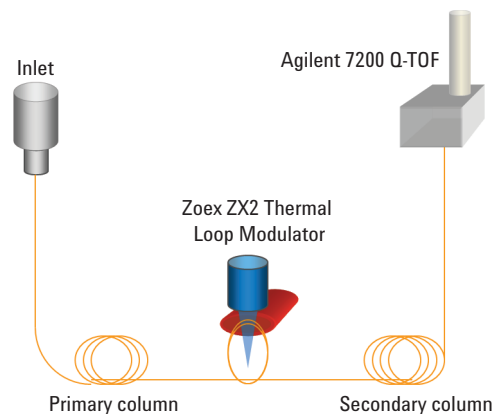


Figure 3. Schematic representation of the Zoex ZX2 Thermal Loop Modulator.

Table 1. Agilent 7890B GC System Coupled to an Agilent 7200 Series GC/Q-TOF MS Run Conditions

GC conditions	
Primary column	Agilent HP-5MS UI, 15 m × 0.25 mm, 0.25 μm film
Secondary column	SGE BPX-50, 3.25 m × 0.1 mm, 0.1 μm film (including 1.0 m as the modulation loop)
Injection volume	1 μL
Split ratio	15:1
Split/Splitless inlet	
temperature	280 °C
Oven temperature program	60 °C 3 °C/min to 310 °C
Carrier gas	Helium at 1.2 mL/min constant flow
Thermal modulation conditions	
Thermal modulation system	ZOEX ZX2
Modulation period	6.8 seconds
Cold jet flow	13 L/min
Hot jet temperature	375 °C
Hot jet duration	320 msec
Q-TOF MS conditions	
Transfer line temperature	310 °C
Ionization mode	EI, PCI
Source temperature	300 °C
Quadrupole temperature	150 °C
Mass range	60 to 650 <i>m/z</i>
Spectral acquisition rate	50 Hz
Emission current	35 μA

Sample preparation

Wildtype (WT) and $\Delta nut1$, $\Delta tps1$, and $\Delta mdt1$ mutant strains of *M. oryzae* were grown in complete media for 48 hours before switching the fungal mycelial mats to grow under minimal media shake conditions in the presence of 1% (w/v) glucose and 10 mM nitrate as sole carbon and nitrogen sources, respectively. Mycelial tissue samples were collected, lyophilized, and ground in liquid nitrogen. The metabolites were extracted using a mixture of methanol:chloroform:water (1:2.5:1, v/v/v). Internal standard (d_{27} -myristic acid) was added to each sample. The extracts were dried under vacuum and derivatized by methoximation followed by silylation with MSTFA + 1% TMCS.

Data processing and statistical analysis

The data were acquired using Agilent MassHunter acquisition software. The MassHunter data files were then imported into GC Image software (GC Image, LLC) for visualization and further processing of the two-dimensional GCxGC data [4].

Image Investigator software (GC Image, LLC) was used for automated and interactive multivariate analyses of multisample datasets for sample classification, fingerprinting, and marker compound discovery. MassHunter Qualitative Analysis (B.07) accurate mass tools, such as the Molecular Formula Generator tool, were used to identify additional unknown compounds.

Results and Discussion

GCxGC feature finding

The MassHunter data files were imported into GC Image for further processing. Each chromatogram was analyzed using a template comprising:

- Peaks common to all chromatograms (“reliable peaks”) for image alignment purposes
- Peak-region features of a composite chromatogram for quantitative image comparison

Reliable peaks were determined from the bidirectional pairwise matching of all possible pairs of chromatograms [5]. The peak-region features were delineated by peak detection in the composite chromatogram created by registering and summing all chromatograms (Figure 4).

GCxGC statistical analysis and library search

The total ion chromatograms (TICs) in each peak region were used to compute the Fisher Discriminant Ratio (FDR) between classes for each feature derived from a composite chromatogram.

Initial compound identification was performed in GC Image by spectral comparison with the NIST14 EI library, taking into consideration linear retention index (RI) values.

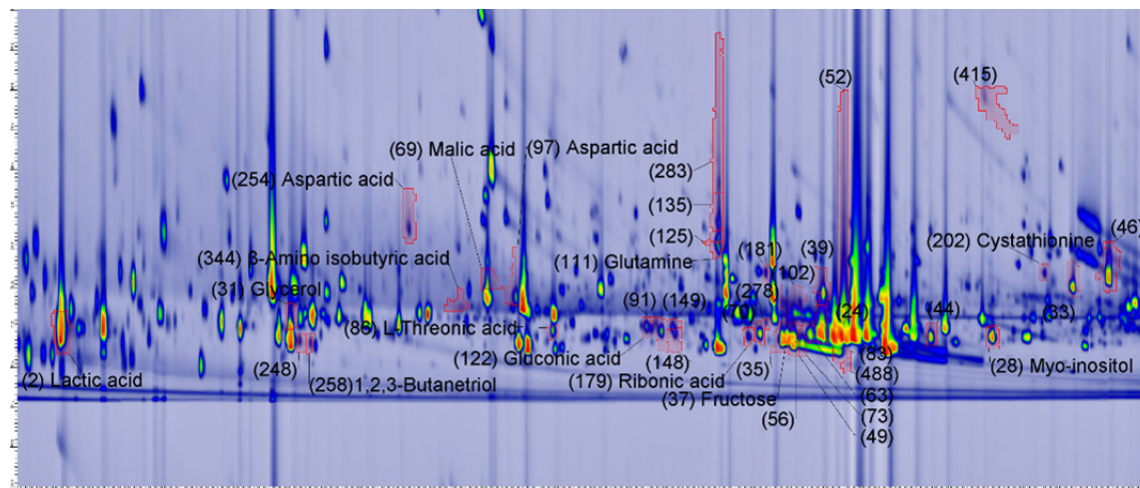


Figure 4. Composite 2D chromatogram displayed in GC image software and denoting some of the identified metabolomic biomarkers.

Identification of unknowns and confirmation of the tentative hits

Two ionization modes were used to identify unknowns. Electron ionization (EI) provided fragment information useful for identification using NIST14 library matching (Figure 5). Many metabolites had molecular ion adducts in positive chemical ionization (PCI) mode with methane as a reagent gas, providing validation of tentative hits (Figure 5).

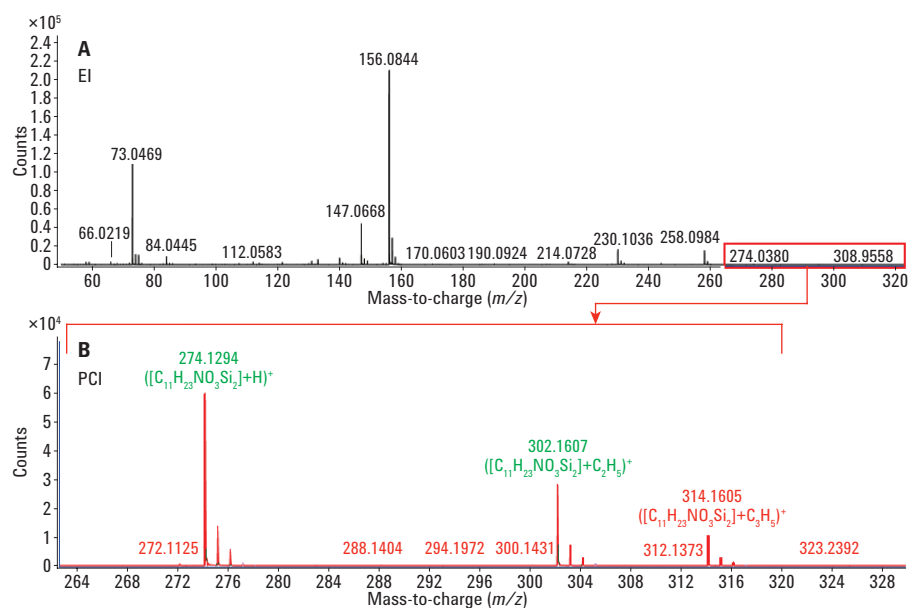


Figure 5. EI spectrum (A) of tentatively identified pyroglutamic acid and its annotated MI cluster obtained with methane PCI (B), used as validation for the identification of this hit.

MassHunter Qualitative analysis accurate mass tools were used to identify metabolites that varied in abundance between WT and mutant strains, using both EI and PCI accurate mass data (Table 2). Molecular Formula Generator (MFG) was used to derive formulae for these metabolites, based on the accurate mass data. Average mass error for the (M+H) ions of these compounds was around 1 ppm. These metabolites exhibited the largest degree of variation between fungal strains, as measured by the FDR determined in GC Image software.

Table 2. Identified Metabolites Exhibiting the Largest Degree of Variation* Between Strains with Confirmed Accurate Mass of (M+H)⁺ in PCI

Compound ID	Formula of derivatized MI	(M+H) m/z	Calculated (M+H) m/z	Mass error (PCI ppm)	M+1 Isotope abundance error, %
Cystathionine	([C ₁₉ H ₄₆ N ₂ O ₄ SSi ₄] ⁺ H)	511.233	511.2328	0.35	2.20
Glutamine	([C ₁₄ H ₃₄ N ₂ O ₃ Si ₃] ⁺ H)	363.1956	363.195	1.50	4.10
Ribonic acid	([C ₂₀ H ₅₀ O ₆ Si ₅] ⁺ H)	527.2536	527.2526	1.77	N/A
Myo-inositol	([C ₂₄ H ₆₀ O ₈ Si ₆] ⁺ H)	613.3079	613.3078	0.14	N/A
glycerol	([C ₁₂ H ₃₂ O ₃ Si ₃] ⁺ H)	309.1731	309.1732	-0.22	2.20
Malic acid	([C ₁₃ H ₃₀ O ₅ Si ₃] ⁺ H)	351.1485	351.1474	3.13	3.70
Aspartic acid	([C ₁₃ H ₃₁ NO ₄ Si ₃] ⁺ H)	350.1638	350.1634	1.18	2.20
L-Threonic acid	([C ₁₆ H ₄₀ O ₅ Si ₄] ⁺ H)	425.2027	425.2026	0.31	1.70
3-Hydroxyisobutyric acid	([C ₁₀ H ₂₄ O ₃ Si ₂] ⁺ H)	249.1339	249.1337	0.80	0.90
Lactic acid	([C ₉ H ₂₂ O ₃ Si ₂] ⁺ H)	235.1183	235.118	1.27	0.20
L-Leucine	([C ₁₂ H ₂₉ NO ₂ Si ₂] ⁺ H)	276.1807	276.181	-1.01	2.80
Pyroglutamic acid	([C ₁₁ H ₂₃ NO ₃ Si ₂] ⁺ H)	274.1288	274.1289	-0.30	1.00
Fumaric acid	([C ₁₀ H ₂₀ O ₄ Si ₂] ⁺ H)	261.0976	261.0973	1.12	0.80
Glycerol 3-phosphate	([C ₁₅ H ₄₁ O ₆ PSi ₄] ⁺ H)	461.1793	461.1791	0.53	2.10
Pyrophosphate	([C ₁₂ H ₃₆ O ₇ P ₂ Si ₄] ⁺ H)	467.1079	467.1086	-1.60	N/A
L-Glutamic acid	([C ₁₄ H ₃₃ NO ₄ Si ₃] ⁺ H)	364.1793	364.179	0.78	2.10
β-Alanine	([C ₉ H ₂₃ NO ₂ Si ₂] ⁺ H)	234.1342	234.134	0.88	0.90
α-Hydroxyglutaric acid	([C ₁₄ H ₃₂ O ₅ Si ₃] ⁺ C ₂ H ₅)	393.1953	393.1943	2.41	0.10
2-Aminobutyric acid	([C ₁₀ H ₂₅ NO ₂ Si ₂] ⁺ H)	248.1493	248.1497	-1.52	N/A
Glycine	([C ₁₁ H ₂₉ NO ₂ Si ₃] ⁺ H)	292.1581	292.1579	0.63	0.80
4-hydroxyproline	([C ₁₁ H ₂₅ NO ₃ Si ₂] ⁺ H)	276.1444	276.1446	-0.57	2.60
N-acetyl-L-Glutamic acid	([C ₁₃ H ₂₇ NO ₅ Si ₂] ⁺ H)	334.1503	334.1501	0.83	0.50
Pyruvic acid	([C ₇ H ₁₅ NO ₃ Si] ⁺ H)	190.0897	190.0894	1.37	2.50
Ornithine	([C ₁₄ H ₃₆ N ₂ O ₂ Si ₃] ⁺ H)	349.2153	349.2157	-1.11	1.00
L-Alanine	([C ₉ H ₂₃ NO ₂ Si ₂] ⁺ H)	234.1342	234.134	0.77	1.80
Mevalonic lactone	([C ₉ H ₁₈ O ₃ Si] ⁺ H)	203.1095	203.1098	-1.53	0.70
Average				1.06	1.68

* Fisher Discriminant Ratio ranging from 4 to 143

Conclusions

In this study, GCxGC/Q-TOF MS methodology was used to compare metabolomes of a wild type isolate of *M. oryzae* to nonpathogenic mutant strains resulting from targeted deletion of key metabolic regulatory genes. Consistent with the role of the *nut1* gene in nitrogen metabolism, *mdt1* in carbon metabolism, and *tps1* in integrating carbon and nitrogen metabolism, statistically significant changes in the carbonaceous and nitrogenous compounds identified in each strain were observed. Notable changes include the requirement of a functional Tps1 protein for the formation of glycerol, a metabolite important for turgor generation in the appressorium. These results may provide evidence of how metabolic regulators ensure the correct assimilation of carbon and nitrogen into metabolites important for infection.

References

1. J. Fernandez, R. A. Wilson. "Cells in cells: morphogenetic and metabolic strategies conditioning rice infection by the blast fungus *Magnaporthe oryzae*" *Protoplasma* **251**(1), 37-47 (2014).
2. R. A. Wilson, N. J Talbot. "Under pressure: investigating the biology of plant infection by *Magnaporthe oryzae*" *Nat. Rev. Microbiol.* **7**, 185–195 (2009).
3. J. Fernandez, J. D. Wright, D. Hartline, C. F. Quispe, N. Madayiputhiya, R. A. Wilson. "Principles of Carbon Catabolite Repression in the Rice Blast Fungus: Tps1, Nmr 1-3, and a MATE-Family Pump Regulate Glucose Metabolism During Infection" *PLoS Genet* **8**: e1002673 (2012).
4. S. Reichenbach. "Data acquisition, visualization, and analysis" *In Comprehensive Two Dimensional Gas Chromatography*, Ed. L. Ramos, pp. 77-106, Elsevier, 2009.
5. S. Reichenbach, X. Tian, C. Cordero, Q. Tao. "Features for non-targeted cross-sample analysis with comprehensive two-dimensional chromatography" *J. Chromatogr. A* **1226**, 140-148 (2012).

For More Information

These data represent typical results. For more information on our products and services, visit our Web site at www.agilent.com/chem.

ZOEX CORPORATION

The Comprehensive Two-Dimensional
Gas Chromatography (GC x GC) Specialists

<http://zoex.com/>

www.agilent.com/chem

Agilent shall not be liable for errors contained herein or for incidental or consequential damages in connection with the furnishing, performance, or use of this material.

Information, descriptions, and specifications in this publication are subject to change without notice.

© Agilent Technologies, Inc., 2016
Printed in the USA
February 18, 2016
5991-6518EN



Agilent Technologies